Advanced Physical Research
Vol.7, No.3, 2025, pp.281-291
https://doi.org/10.62476/apr.73281

INFLUENCE OF HETEROATOMS (N AND O) ON THE ELECTRICAL AND THERMOELECTRIC PROPERTIES OF ANTHRACENE MOLECULAR JUNCTION

Hayder Hashim Harib*, **Mohammed Deia Noori**

Department of Physics, College of Sciences, University of Thi-Qar, Thi-Qar, Iraq

Abstract. Thermoelectric energy conversion offers a viable solution to harvesting waste heat and transforming it into usable electrical power. This investigation examines the impact of oxygen and nitrogen heteroatom doping on the structural and functional performance of anthracene-based molecular junctions. This work systematically investigates the influence of impurity type, location, and number. Findings reveal that oxygen incorporation, particularly when localized in the middle ring or with increased impurity number in both the middle and peripheral rings, substantially elevates thermoelectric performance, achieving a peak ZT of 3.5 in the D2O configuration. In contrast, nitrogen doping consistently reduced ZT values, irrespective of the impurity's position or count. The results emphasize that accurately selecting the positioning of heteroatoms is essential for maximizing thermoelectric efficiency.

Keywords: Molecular junctions, Thermoelectric, Seebeck, Quantum interference, PAHS.
Corresponding author: Hayder Hashim Harib, Department of Physics, College of Sciences, University of Thi-Qar, Iraq, Thi-Qar, Iraq, e-mail: *hayder.hashim@utq.edu.iq*
Received: 13 June 2025; Revised: 29 July 2025; Accepted: 23 August 2025; Published: 16 October 2025.

1 Introduction

The ongoing global energy dilemma, propelled by the depletion of fossil fuels and the environmental repercussions of excessive nonrenewable energy consumption, underscores the urgency for sustainable alternatives (Lee et al., 2023; Zhang et al., 2024). Thermoelectric materials have emerged as promising candidates for converting thermal waste into electrical energy, especially since a considerable portion, exceeding 60% of the produced energy, dissipates as heat (d'Angelo et al., 2023; Preesam et al., 2023). Thermoelectric systems offer practical advantages such as being solid-state devices with high scalability and operational stability. Their performance is quantified by the dimensionless figure of merit ZT (He et al., 2024; Lee, 2018). Recent advancements have aimed at enhancing ZT values through molecular engineering approaches, with particular focus on polycyclic aromatic hydrocarbons such as anthracene, known for its structural symmetry and chemical stability (Al-mebir et al., 2021, 2023; McKeown, 1998; Wang et al., 2020).

Grasping the fundamental principles that govern charge transport efficiency in molecules situated within nanogaps presents a significant challenge in the field of molecular electronics (d'Angelo et al., 2023; Huang et al., 2015; Noori & Al-Jobory, 2018; Noori, 2017). In conventional silicon-based electronic devices, the electrical transport characteristics are mainly adjusted by doping the semiconductor materials (O'Driscoll et al., 2021; Yang et al., 2018) while the flow of electrical current is controlled through electrical gating (Fang et al., 2025). A similar strategy involves doping aromatic molecules with heteroatoms to influence their transport characteristics

(Sakban et al., 2020; Wang et al., 2021).

For example, adding oxygen or nitrogen atoms to molecular systems can reduce their bonding molecular orbitals while increasing electron transport capabilities (Lee, 2018; Liu et al., 2015). Heteroatoms can also influence the coupling between the molecule and the electrode, therefore modifying the transport characteristics of the whole device (Feng et al., 2018; Zhao et al., 2024). González et al. (Chen et al., 2023) studied the molecular conductance of pyrimidine-containing molecules and found that double N-substitution has little effect on the molecular conductance (Gümüş & Akbay, 2013; Miguel et al., 2015). They also reported that the conductance of N-substituted anthracene derivatives is comparable to that of the pristine all-carbon anthracene compound (Palomino-Ruiz et al., 2021). Meanwhile, the O-substitution in anthracene increases the molecular conductance (Ulcakar et al., 2020; Zhao et al., 2020).

More importantly, because room-temperature charge transport in molecular systems is governed by quantum mechanics (Wang et al., 2020), introducing heteroatoms into specific atomic sites within molecules can significantly modulate their transport behaviors by tuning various interesting quantum interference (QI) effects (Al-Abboodi et al., 2017; Yanagi et al., 2014). Among the different quantum phenomena in molecular devices, QI has received a lot of interest in recent years (Leary et al., 2018; Noori et al., 2018; Poudel et al., 2008; Preesam et al., 2024).

The modification of QI has concentrated on the impacts of a single heteroatom substitution (O'Driscoll et al., 2021). As a result, it is logical to wonder whether adding numerous heteroatoms to molecular systems might result in novel QI effects that do not exist in molecules with single heteroatoms (Chen et al., 2023; Wang et al., 2021). When an aromatic unit contains more than one heteroatom, adjusting the relative locations of the doping results in a wide range of molecular structures (Gümüş & Akbay, 2013). However, our understanding of the impact of heteroatom substitution on QI remains quite restricted.

This work aims to study the effect of the impurity of a heterogeneous atom of oxygen or nitrogen on an anthracene molecule, and to analyze the role of the location of this impurity within the molecular rings, as well as the effect of increasing the number of impurities at the same sites, on the electronic and thermoelectric properties of the molecule, and exploring the behavior of quantum interference, when the anthracene terminal rings are attached to gold electrodes.

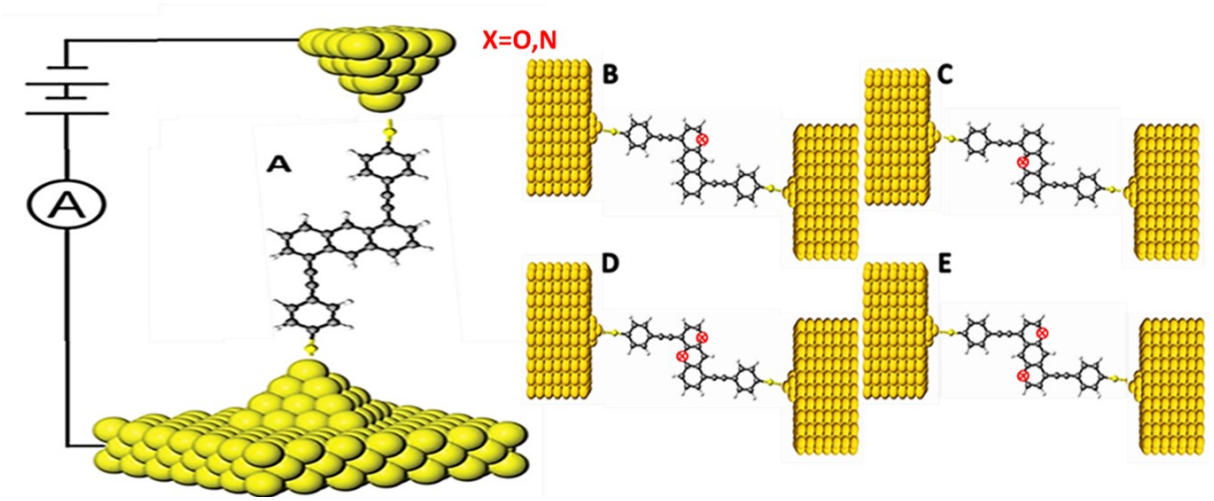

Figure 1: Molecular structures of anthracene-based junctions connected to Au electrodes via thiol linkers attached at the terminal rings (first and third rings). The symbol X denotes a heteroatom (O or N), depending on the configuration. (A) pure anthracene. (B) One X atom at a terminal ring (BO or BN). (C) One X atom at the middle ring (CO or CN). (D) Two X atoms at the middle and a terminal ring (D2O or D2N). (E) Two X atoms at both terminal rings (E2O or E2N). Impurities in the terminal rings that are connected to gold atoms.

2 Method

All thermoelectric calculations in this study were performed at room temperature (300 K). The geometry of each structure investigated in this work was relaxed to a force tolerance of 10 meV/Åusing the SIESTA (Soler et al., 2002) implementation of DFT (Khudhair & Hanoon, 2021a,b) with a double-ζ polarized basis set (DZP) and the Generalized Gradient Approximation (GGA) (Ferrer et al., 2014) functional. To calculate the electrical and thermoelectric properties of all the anthracene molecular junctions shown in Fig. 1, the underlying mean-field Hamiltonian (H) was combined with the quantum transport code Gollum (Perdew et al., 1996) to calculate the transmission coefficient $T(E)$. The electrical conductance G was computed by using the Landauer formula. We compute the thermopower S over a wide range of Fermi energies by using the equation. The Seebeck coefficient is defined as: The Seebeck coefficient is defined as:

$$S(E) = -\frac{\Delta V}{\Delta T} = -\frac{1}{eT}\frac{L_1}{L_0} \tag{1}$$

where T is the temperature, e is the electron charge, and L_n can be calculated as:

$$L_n = \int_{-\infty}^{\infty} (E - E_F)^n T(E) \left(-\frac{\partial f(E,T)}{\partial E}\right) dE \tag{2}$$

Electrical conductance G is given by:

$$G = \frac{2e}{h} L_0 \tag{3}$$

Thermal conductance κ is given by:

$$\kappa = \frac{2}{h}\frac{1}{T}\left(L_2 - \frac{L_1^2}{L_0}\right) \tag{4}$$

The quantity that defines thermoelectric efficiency is ZT. The ZT is a dimensionless figure of merit proportional to electric conductance G, the square of the Seebeck coefficient S, and inversely proportional to thermal conductance κ.

Electronic contribution to the figure of merit ZT:

$$ZT = \frac{1}{\left(\frac{L_0 L_2}{L_1^2}\right) - 1} \tag{5}$$

This study considers only the electronic contribution to thermoelectric transport. The phonon thermal conductance was not included in the ZT calculation. This simplification is consistent with earlier studies on π-conjugated molecular junctions (Al-Mohana et al., 2024), where the electronic contribution was shown to dominate at room temperature and under conditions where vibrational coupling to electrodes is weak. Nevertheless, the absence of phonon transport is acknowledged as a limitation in the present study.

3 Results and Discussion

Systematically interpret the results presented in this work. Table 1 categorizes the studied anthracene-based molecular junctions according to dopant type, number, and location within the molecular structure. This classification facilitates a clearer interpretation of the subsequent results and graphical representations.

Table 1: Summary of investigated molecular configurations.

Label	**Dopant Type**	**Number of Dopants**	**Doping Positions**	**Description**
A	None	0	—	pure anthracene
BO	O	1	Terminal ring	One oxygen atom at the terminal site
BN	N	1	Terminal ring	One nitrogen atom at the terminal site
CO	O	1	Middle ring	One oxygen atom in the middle ring
CN	N	1	Middle ring	One nitrogen atom in the middle ring
D2O	O	2	Middle + terminal ring	Two oxygen atoms at the middle and terminal positions
D2N	N	2	Middle + terminal ring	Two nitrogen atoms at the middle and terminal positions
E2O	O	2	Both terminal rings	Two oxygen atoms at both terminal rings
E2N	N	2	Both terminal rings	Two nitrogen atoms at both terminal rings

The analysis of the electronic and thermoelectric behavior of the selected systems begins with the calculation of the electronic transmission coefficient $T(E)$ for all configurations listed in Table 1 and depicted in Fig. 1. Fig. 2 displays the energy-dependent transmission spectra for both pristine and heteroatom-doped anthracene molecular junctions.

Specifically, Fig. 2a compares the transmission coefficients of pristine anthracene (A) with systems containing a single heteroatom dopant at the terminal ring (BO and BN). Fig. 2b shows the results for configurations with a single dopant located in the middle ring (CO and CN). Fig. 2c displays the transmission for molecules doped with two heteroatoms, one in the middle and one in the terminal ring (D2O and D2N). Finally, Fig. 2d presents the systems with two dopants placed symmetrically at both terminal rings (E2O and E2N).

These results demonstrate the significant influence of heteroatom type and position on the transmission spectra, and thus on the charge transport characteristics of anthracene-based junctions.

The computational investigation commenced by substituting a one-carbon atom within the anthracene molecule with oxygen or nitrogen. Introducing these dopants led to notable changes in bond lengths. C–O bonds became longer, while C-N bonds showed contraction. In contrast, the C-C bonds experience a slight contraction. Upon introducing oxygen impurity, it became evident that the inherent symmetry of the two carbon sub-lattices was disrupted, leading to a notable reduction in the energy gap as depicted in Fig. 2(a-d), in which the narrowest energy gap was achieved by doping anthracene with one oxygen impurity, predominantly at the terminal aromatic rings. The insertion of a single nitrogen impurity into the anthracene structure resulted in just a little change in the energy gap when compared to pure anthracene.

To investigate the impact of the increased number of impurities on the anthracene configuration, the simulations were expanded to include two impurity atoms, either oxygen or nitrogen Gümüş & Akbay (2013). This methodology enabled a full assessment of how alternative dopants and configurations affect the system's electrical characteristics. The results showed that increasing the number of impurities from one to two leads to greater disruption of the π network, causing significant changes in the energy gap and quantum interference patterns. This has resulted in shifts in the behaviour of electronic transport, depending on the locus of impurities, highlighting the importance of controlling the number and location of the distortion atoms to adjust the electronic properties of the molecule, as depicted in Fig. 2.

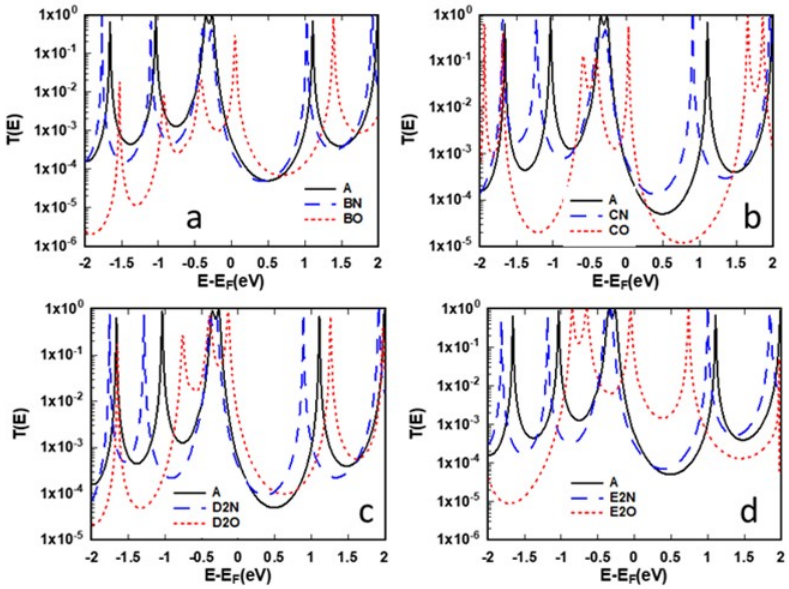

Figure 2: Electronic transmission coefficient T(E) as a function of energy for all molecular junctions that appear in Fig. 1

Figure 3a–d presents the room-temperature electrical conductance as a function of energy for each studied molecular structure. The introduction of oxygen atoms into the anthracene framework led to a noticeable enhancement in conductance. This improvement is primarily attributed to the strong electronegativity of oxygen, which promotes a redistribution of electron density within the π-conjugated system. This redistribution enhances charge transport by elevating the transmission coefficient. In contrast, nitrogen doping exhibited a much weaker influence on conductance. The nonbonding electron pair associated with nitrogen does not actively engage in charge transport (Eklund & Karttunen, 2022), resulting in only minor modifications to the electronic structure. Consequently, the density of states near the Fermi level remains largely unaffected, and the electrical performance of the system remains close to that of the pure anthracene molecule. These findings underscore the distinct roles of heteroatoms in modulating molecular transport behavior.

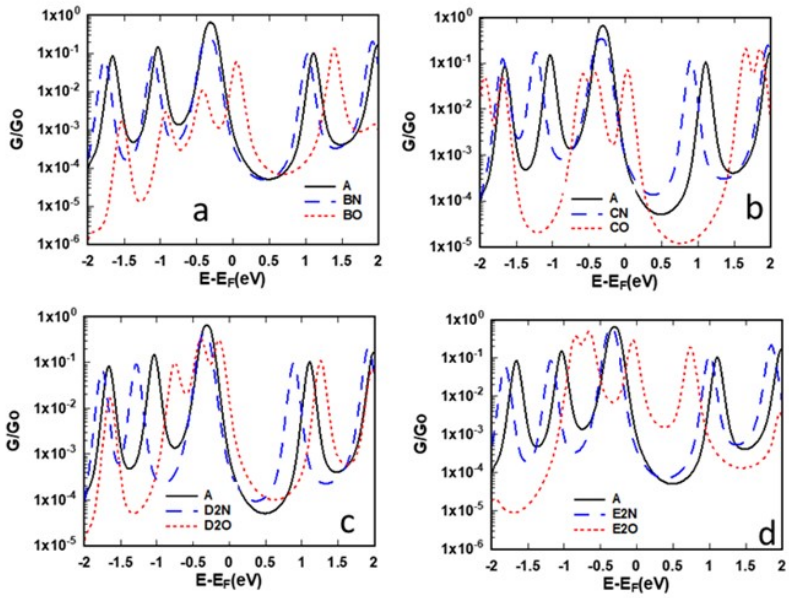

Figure 3: Electrical conductance as a function of energy for all molecular junctions that appear in Fig. 1

Figure 4 shows the thermal conductivity (κ) as a function of energy for all anthracene molecular junctions. Figure 4a-d shows that, similar to the electrical conductance case, the doping with oxygen impurity shows high values of thermal conductivity compared with nitrogen doping. This improvement is due to the electronegative nature of oxygen, which promotes electronic transmission without causing localized disturbances that hinder energy transfer. In turn, introducing nitrogen leads to the formation of local states within the π lattice, which hinder heat transfer through the molecule. These states act as barriers to electronic transmission, which explains the low thermal conductivity in nitrogen-doped samples as shown in Fig. 4a-d.

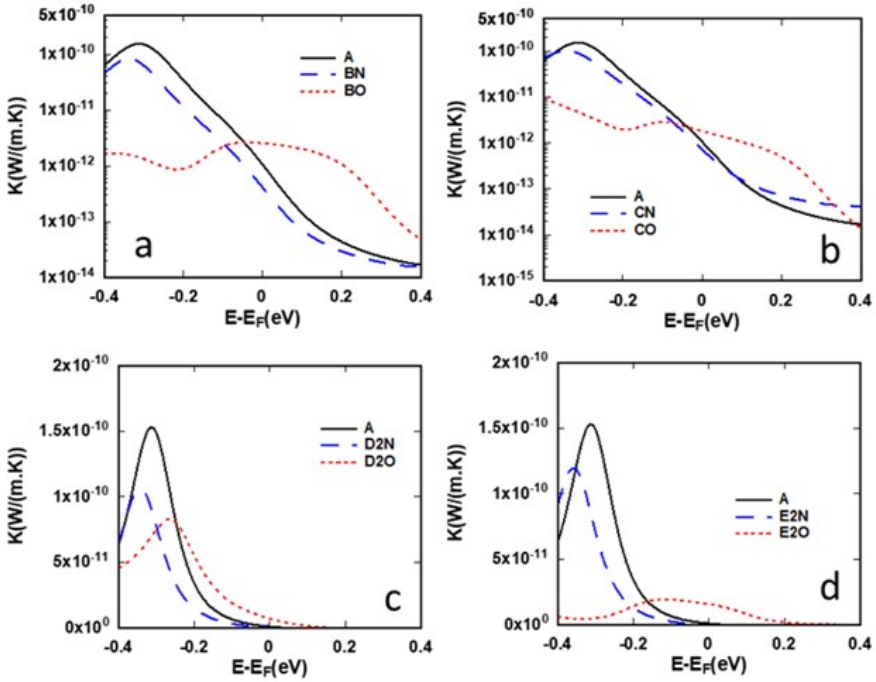

Figure 4: Thermal conductivity as a function of energy for all molecular junctions that appear in Fig.1

Figure 5 shows the Seebeck coefficient S as a function of energy at 300 K for each structure under investigation. Fig. 5a–d shows the observed improvement in Seebeck's modulus when the anthracene molecule is distorted with oxygen atoms due to the high electronegativity of these atoms, which alters the electron density distribution, to increase asymmetry around the Fermi level and enhance thermopower. This variation in state density contributes to raising the Seebeck coefficient. In contrast, the doping of the molecule anthracene with nitrogen atoms leads to the formation of localised electronic states that act as traps for charge carriers, hindering their flow and impairing the Seebeck coefficient. Therefore, the fundamental differences in the electronic and structural effects of oxygen and nitrogen are a direct cause of the different performance of the two systems in terms of thermoelectric efficiency.

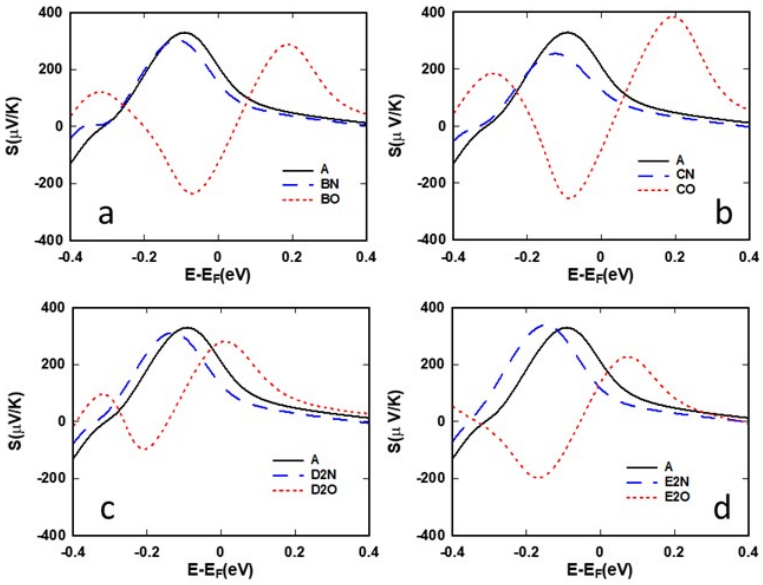

Figure 5: Seebeck coefficient as a function of energy for all molecular junctions that appear in Fig1

Figure 6 depicts the electrical figure of merit ZT for all configurations over a range of energies. ZT, the thermoelectric figure of merit, is calculated by combining conductance (G), Seebeck coefficient (S), and thermal conductivity (κ). The results demonstrate that oxygen doping enhances the material's thermoelectric figure of merit ZT, as seen in Figure 6a-d. This rise positively affects the material's overall performance in thermoelectric applications. On the contrary, nitrogen doping lowers the material's thermoelectric figure of merit ZT. The data shown in Figure 6a–d indicate that the D2O structure, which includes two oxygen atoms placed in the middle ring and the terminal ring directly connected to the gold electrodes, achieved the highest recorded value of ZT of about 3.5 at 0.0 V, in conjunction with high electrical conductivity, and the E2O structure involving two oxygen atoms placed in the terminal rings directly connected to the gold electrodes achieved a value for ZT of about 2.5 at the same energy, supporting the hypothesis that the oxygen impurities at strategic locations within the molecule are a critical factor in improving the thermoelectric performance of organic molecules.

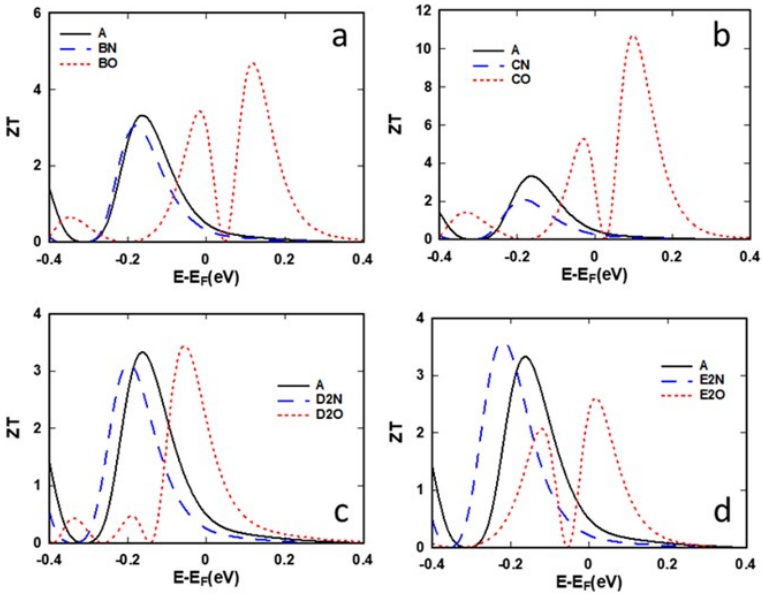

Figure 6: ZT (the efficiency of thermoelectrical materials) as a function of energy for all molecular junctions that appear in Fig. 1

Previous studies on PAH-based molecular junctions, including pristine and functionalized anthracene systems, have typically reported ZT values ranging from 0.1 to 1.5, depending on the molecular structure, contact geometry, and linker groups (Zhao et al., 2024; Noori et al., 2018; Wang et al., 2021). For example, Noori et al. (Noori et al., 2018) reported a ZT $\approx$ 0.8 for stable-radical-modified graphene nanoconstrictions, while O'Driscoll et al. (O'Driscoll et al., 2021) obtained ZT values below 1.5 for N-substituted anthracene derivatives.

In contrast, the D2O configuration in our study, featuring two oxygen atoms placed at the central and terminal rings achieved a maximum ZT of approximately 3.5, while the E2O structure yielded ZT $\approx$ 2.5. This substantial enhancement emphasizes the critical influence of heteroatom positioning in tuning quantum interference and optimizing the thermoelectric response in π-conjugated systems.

4 Conclusion

We used DFT calculations to analyze the effect of atomic impurities on the thermoelectric properties of an anthracene molecule, focusing on the type, location, and number of impurities. The results showed that oxygen atoms enhance thermoelectric performance compared to nitrogen atoms, due to oxygen's electronegativity, which improves the Seebeck coefficient and electron transport efficiency. Moreover, the impurity's position within the aromatic ring critically affects thermoelectric performance, as its position in the middle ring enhances the value of the figure of merit (ZT) compared to the terminal sites. Additionally, introducing multiple oxygen atoms, particularly in both the middle and terminal rings bonded to gold electrodes, resulted in a significant rise in the ZT value, reaching a peak of 3.5 in the D2O configuration. Conversely, nitrogen doping consistently led to diminished ZT values, regardless of its position or number, due to its limited influence on electronic transport mechanisms. These results reinforce the critical role of dopant type, position, and number in optimizing thermoelectric performance as a key approach for optimizing the thermoelectric performance of organic molecular systems.

Acknowledgement The authors would like to thank the Department of Physics, College of Sciences, University of Thi-Qar for their support. This research received no specific grant from any funding agency in the public, commercial, or not-for-profit sectors.

References

Al-Abboodi, M.H., Ajeel, F.N., & Khudhair, A.M. (2017). Influence of oxygen impurities on the electronic properties of graphene nanoflakes. *Physica E: Low-Dimensional Systems and Nanostructures*, *88*, 1–5.

Al-mebir, A.A.K., Noori, M.D., & Kadhim, B. B. (2021). Tuning the Electrical and Thermoelectric Properties of Phthalocyanine and Metallo-Phthalocyanine Molecular Junction. In *Journal of Physics: Conference Series* (Vol. 1999, p. 012036). IOP Publishing.

Al-mebir, A.A.K., Noori, M.D., & Kadhim, B.B. (2023). Investigation of the electric and thermoelectric properties of metallo-phthalocyanine molecular junctions with planar and axial configuration. In *AIP Conference Proceedings* (Vol. 2457). AIP Publishing.

Al-Mohana, S.M.S., Najeeb, H.N., Al-Utayjawee, R.M., Babaei, F., & Al-Owaedi, O.A. (2024). Theoretical investigation of thermoelectric properties of methyl blue-based molecular junctions. *RSC Advances*, *14*(33), 23699–23709.

Chen, Z., Wu, S., Lin, J., Chen, L., Cao, J., Shao, X., ... Zhang, H. (2023). Modulating Quantum Interference Between Destructive and Constructive States in Double N-Substituted Single Molecule Junctions. *Advanced Electronic Materials, 9*(2), 2201024.

d'Angelo, M., Galassi, C., & Lecis, N. (2023). Thermoelectric Materials and Applications: A Review. *Energies*, *16*(17), 6409.

Eklund, K., Karttunen, A.J. (2022). Effect of the Dopant Configuration on the Electronic Transport Properties of Nitrogen-Doped Carbon Nanotubes. *Nanomaterials*, *12*(2). doi:10.3390/nano12020199

Fang, C., Li, Y., Wang, S., Liang, M., Yan, C., Liu, J., & Hong, W. (2025). Thermoelectric and Thermal Properties of Molecular Junctions: Mechanisms, Characterizations and Applications. *Chemical Communications*.

Feng, J., Dong, H., Pang, B., Shao, F., Zhang, C., Yu, L., & Dong, L. (2018). Theoretical study on the optical and electronic properties of graphene quantum dots doped with heteroatoms. *Physical Chemistry Chemical Physics*, *20*(22), 15244–15252.

Ferrer, J., Lambert, C.J., García-Suárez, V.M., Manrique, D.Z., Visontai, D., Oroszlány, L., ... Gillemot, K. (2014). GOLLUM: a next-generation simulation tool for electron, thermal and spin transport. *New Journal of Physics*, *16*(9), 093029.

Gümüş, S., Akbay, M. (2013). A Computational Study on Substituted and Unsubstituted Mono and Diazaanthracenes. *Polycyclic Aromatic Compounds*, *33*(5), 519–532.

He, J., Li, K., Jia, L., Zhu, Y., Zhang, H., & Linghu, J. (2024). Advances in the applications of thermoelectric generators. *Applied Thermal Engineering*, *236*, 121813.

Huang, C., Rudnev, A.V., Hong, W., & Wandlowski, T. (2015). Break junction under electrochemical gating: testbed for single-molecule electronics. *Chemical Society Reviews*, *44*(4), 889–901.

Khudhair, A.T., Hanoon, F.H. (2021a). A DFT Study of The Sensing and Adsorption of Graphene Nanoribbons for DNA Sequencing. *University of Thi-Qar Journal of Science*, *8*(1), 141–147.

Khudhair, A.T., Hanoon, F.H. (2021b). Theoretical Study of Carbon Nanotube toward Adenine Sensing: DFT Study. *University of Thi-Qar Journal of Science*, *8*(1), 136–140.

Leary, E., Limburg, B., Alanazy, A., Sangtarash, S., Grace, I., Swada, K., ... Nichols, R. J. (2018). Bias-Driven Conductance Increase with Length in Porphyrin Tapes. *Journal of the American Chemical Society*, *140*(40), 12877–12883. doi:10.1021/jacs.8b06338

Lee, H. (2018). *Thermoelectrics: Design and Materials*. Springer.

Lee, J., Kim, S., You, S., & Park, Y.K. (2023). Bioenergy generation from thermochemical conversion of lignocellulosic biomass-based integrated renewable energy systems. *Renewable and Sustainable Energy Reviews*, *178*, 113240.

Liu, K., Song, C.-L., Zhou, Y.-C., Zhou, X.-Y., Pan, X.-J., Cao, L.-Y., ... Zhang, H.-L. (2015). Tuning the ambipolar charge transport properties of N-heteropentacenes by their frontier molecular orbital energy levels. *Journal of Materials Chemistry C*, *3*(16), 4188–4196.

McKeown, N.B. (1998). *Phthalocyanine materials: synthesis, structure and function*. Cambridge University Press.

Miguel, D., Alvarez de Cienfuegos, L., Martín-Lasanta, A., Morcillo, S.P., Zotti, L.A., Leary, E., ... Cárdenas, D.J. (2015). Toward multiple conductance pathways with heterocycle-based oligo (phenyleneethynylene) derivatives. *Journal of the American Chemical Society*, *137*(43), 13818–13826.

Noori, M., Sadeghi, H., & Lambert, C.J. (2018). Stable-radicals increase the conductance and Seebeck coefficient of graphene nanoconstrictions. *Nanoscale*, *10*(40), 19220–19223. doi:10.1039/c8nr04869j

Noori, M.D., Al-Jobory, A.A. (2018). Tuning the Thermoelectric Properties of Ferrocene Molecular Junctions. In *IOP Conference Series: Materials Science and Engineering* (Vol. 454, p. 012143). IOP Publishing.

Noori, M.D. (2017). *Quantum Theory of Electron Transport Through Photo-Synthetic Porphyrins*. Lancaster University (United Kingdom).

O'Driscoll, L.J., Sangtarash, S., Xu, W., Daaoub, A., Hong, W., Sadeghi, H., & Bryce, M.R. (2021). Heteroatom Effects on Quantum Interference in Molecular Junctions: Modulating Antiresonances by Molecular Design. *The Journal of Physical Chemistry C*, *125*(31), 17385–17391.

Palomino-Ruiz, L., Rodríguez-González, S., Fallaque, J.G., Márquez, I.R., Agraït, N., Díaz, C., ... Martín, F. (2021). Single-molecule conductance of 1, 4-azaborine derivatives as models of BN-doped PAHs. *Angewandte Chemie International Edition*, *60*(12), 6609–6616.

Perdew, J.P., Burke, K., & Ernzerhof, M. (1996). Generalized Gradient Approximation Made Simple. *Physical Review Letters, 77*(18), 3865.

Poudel, B., Hao, Q., Ma, Y., Lan, Y., Minnich, A., Yu, B., ... Ren, Z. (2008). High-thermoelectric performance of nanostructured bismuth antimony telluride bulk alloys. *Science*, *320*(5876), 634–638. doi:10.1126/science.1156446

Preesam, D., Noori, M., & Moghaddam, H. (2023). The Effect of Linker Group on Thermoelectric Properties of Dimer Zinc Porphyrin-Based Molecular Junctions. *University of Thi-Qar Journal of Science*, *10*(2), 177–180.

Preesam, D.S., Milani Moghaddam, H., & Noori, M.D. (2024). Enhanced thermoelectric properties of zinc porphyrin dimers-based molecular devices. *The European Physical Journal D*, *78*(11), 1–5.

Sakban, R.H., Noori, M.D., & Abdulalmohsin, S.M. (2020). Radical Enhancement Electric and Thermoelectric Efficiency of Graphene Nano constrictions. *Solid State Technology*, *63*(1), 1788–1793.

Soler, J.M., Artacho, E., Gale, J.D., García, A., Junquera, J., Ordejón, P., & Sánchez-Portal, D. (2002). The SIESTA method for ab initio order-N materials simulation. *Journal of Physics: Condensed Matter*, *14*(11), 2745.

Ulčakar, L., Rejec, T., Kokalj, J., Sangtarash, S., Sadeghi, H., Ramšak, A., ... Lambert, C.J. (2020). On the resilience of magic number theory for conductance ratios of aromatic molecules. *Scientific Reports*, *10*(1), 3478.

Wang, X., Bennett, T.L.R., Ismael, A., Wilkinson, L.A., Hamill, J., White, A.J.P., ... Robinson, B. J. (2020). Scale-up of room-temperature constructive quantum interference from single molecules to self-assembled molecular-electronic films. *Journal of the American Chemical Society*, *142*(19), 8555–8560.

Wang, Y.-H., Yan, F., Li, D.-F., Xi, Y.-F., Cao, R., Zheng, J.-F., ... Zhou, X.-S. (2021). Enhanced gating performance of single-molecule conductance by heterocyclic molecules. *The Journal of Physical Chemistry Letters*, *12*(2), 758–763.

Yanagi, K., Kanda, S., Oshima, Y., Kitamura, Y., Kawai, H., Yamamoto, T., ... Maniwa, Y. (2014). Tuning of the thermoelectric properties of one-dimensional material networks by electric double layer techniques using ionic liquids. *Nano Letters*, *14*(11), 6437–6442. doi:10.1021/nl502982f

Yang, Y., Gantenbein, M., Alqorashi, A., Wei, J., Sangtarash, S., Hu, D., ... Chen, L. (2018). Heteroatom-induced molecular asymmetry tunes quantum interference in charge transport through single-molecule junctions. *The Journal of Physical Chemistry C*, *122*(26), 14965–14970.

Zhang, Y., Li, L., Sadiq, M., & Chien, F. (2024). The impact of non-renewable energy production and energy usage on carbon emissions: evidence from China. *Energy & Environment*, *35*(4), 2248–2269.

Zhao, Y., Zhang, G., Wen, L., Wang, S., Wang, Y., Li, Y., & Ge, M. (2024). Experimental study on thermoelectric characteristics of intermediate fluid thermoelectric generator. *Applied Energy*, *365*, 123263.

Zhao, Z.-H., Wang, L., Li, S., Zhang, W.-D., He, G., Wang, D., ... Wan, L.-J. (2020). Single-molecule conductance through an isoelectronic B–N substituted phenanthrene junction. *Journal of the American Chemical Society*, *142*(18), 8068–8073.